THE NUMERICAL SOLUTION OF PRESSURE OSCILLATIONS IN AN OPEN CAVITY

by

W. L. Hankey and J. S. Shang
Air Force Flight Dynamics Laboratory
Wright-Patterson AFB, Ohio

Open cavities on aircraft exposed to high speed flow, such as bomb bays can give rise to intense self-induced pressure oscillations. The amplitude of these oscillations, under certain flight conditions, can cause structural damage. Substantial experimental and analytical efforts have investigated these pressure fluctuations, resulting in some understanding of the complex interaction of the external shear layer and cavity acoustical disturbances. However, no numerical computations have been obtained for the complete governing fluid mechanical equations. The purpose of this study is to obtain numerical solutions of the Navier-Stokes equations for an open cavity in order to provide a new tool for the analysis of this phenomenon.

Manuscript Received June 1979. This work performed under AFFDL Work Unit No. 2306N603.

NOMENCLATURE

a	=	speed of sound
A	=	coefficient in pressure perturbation equation
c	=	complex propagation speed
C_p	=	specific heat at constant pressure
D	=	cavity depth
e	=	specific internal energy
E, F	=	vector fluxes
f	=	frequency of wave
k	=	c_1/U_∞ propagation velocity ratio
L	=	cavity length
m	=	mode number
M	=	Mach number
n	=	mode number
p	=	pressure
$\dot{q}$	=	heat transfer rate
R	=	gas constant
Re	=	Reynolds number
t	=	time
T	=	temperature
u, v	=	velocity components in Cartesian frame
U	=	vector of dependent variables
x, y	=	Cartesian coordinates
α	=	$2\pi\delta/\lambda$ dimensionless wave number
γ	=	ratio of specific heats
δ	=	shear layer thickness

λ	=	wave length
μ	=	viscosity (molecular and eddy)
ρ	=	density
σ	=	normal stress
τ	=	viscous shear stress
ϕ	=	amplitude of perturvation velocity
ω	=	$2\pi f$ frequency

Subscripts

∞	=	freestream condition
o	=	stagnation condition
w	=	wall condition
r	=	real part
i	=	imaginary part
1	=	forward traveling wave
2	=	rearward traveling wave

Superscripts

$'$	=	instantaneous perturbation variable
$-$	=	vector

I. Background

As early as 1955, Krishnamurty[1] investigated flow induced pressure oscillations in open cavities. Other investigators[2,3,4,5,6,7,8,9] have conducted extensive research in an attempt to understand the physical mechanisms. Heller and Bliss[3] used a water table to simulate supersonic airflow over open cavities. They found that the inherently unstable shear layer fluctuates, causing periodic mass addition and expulsion from the cavity (Figure 1). When the rear reattachment point of the shear layer enters the cavity, a stagnation point is created; thus increasing the local cavity pressure. This mass addition creates a traveling pressure wave (as in a shock tube), which moves forward in the cavity (at supersonic speed relative to free stream), trailing an oblique shock in the free stream. When the traveling shock wave reflects from the forward bulkhead, a pressure doubling occurs in the cavity while disturbances in the external flow are not reflected, and thus a pressure jump across the shear layer deflects the shear layer. The reflected traveling shock wave in the cavity is now moving at subsonic speed relative to the free stream, hence, generates no oblique shock wave in the free stream. As the cavity traveling shock wave approaches the rear bulkhead, the shear layer bulges outward, and mass is ejected out of the cavity. The entire process then repeats itself in a periodic fashion.

Thus, sufficient experience from such extensive measurements exists so that a qualitative description of the flow process can be obtained. However, a quantitative prediction method does not exist which is the motivation for the present investigation.

To study self-induced pressure oscillations in an open cavity, an analytic study was first accomplished, followed by a numerical computation of the Navier-Stokes equations and a comparison with previous experimental investigations.

II. Analytical Study

Consider a system of traveling waves which produce the wave-diagram (x,t) shown in Figure 2. A resonant situation arises when a forcing function excites the shear layer in the frequency range where amplification is possible. The disturbances will grow until a limit cycle is reached due to viscous dissipation. A standing wave exists in the cavity when both the upstream and downstream traveling waves are synchronized. This wave pattern of Figure 2 may be approximated by considering forward and rearward traveling pressure waves of equal intensity but different propagation velocities and wave numbers.

$$p' = Ae^{i\alpha_1(x - c_1 t)} + Ae^{i\alpha_2(-x - c_2 t)} \tag{1}$$

The frequency of the pressure pulse can be determined directly from the wave diagram.

$$\frac{m}{f} = \frac{L}{c_1} + \frac{L}{c_2} \tag{2}$$

where m is the number of waves or mode number.

From observation of cavity oscillations the rearward traveling wave (α_2) is known to be an acoustical disturbance traveling at the speed of sound in the cavity.

$$c_2 = U_\infty \sqrt{1 + 0.2M_\infty^2}\; M_\infty^{-1}$$

The progagation speed of the forward traveling wave has been observed to be about half of the free stream value[6].

$$\frac{c_1}{U_\infty} \equiv k \sim 1/2 \tag{4}$$

The frequency can be evaulated by using these results.

$$f = \frac{mU_\infty}{L(M_o + k^{-1})} \qquad \text{Rossiter's Formula (Ref 4)} \tag{5}$$

This equation have been used successfully for determining cavity resonant frequencies but no satisfactory prediction method has been available for determining the disturbance intensity of the different modes.

The mode shape of these standing waves can also be deduced from the preceding equations. For a standing wave to occur both waves must possess the same frequency.

$$\omega = \alpha_1 c_1 = \alpha_2 c_2 = 2\pi f \tag{6}$$

Combining this result with equation 2 produces the following relationship:

$$\alpha_1 + \alpha_2 = \frac{2\pi m}{L} \tag{7}$$

The mode shape may be obtained by utilizing this information in the pressure equation (equation 1) and computing the rms value of pressure over a complete cycle.

$$p_{rms} = A(1 + \cos\,(\alpha_1 + \alpha_2)x)^{1/2}$$
$$p_{rms} = A\left|\cos \frac{m\pi x}{L}\right| \tag{8}$$

These patterns have been documented in Ref 3. Nodes will occur when

$$\frac{m\pi x}{L} = n\frac{\pi}{2}\,; \qquad n = \text{odd}$$

Mode m	Nodes n		
	1	3	5
1	1/2	---	---
2	1/4	3/4	---
3	1/6	3/6	5/6

Table I Node Location for Various Modes

III. Stability Analysis

A necessary condition for resonance is that one of the waves must be unstable for the oscillation to persist, otherwise the disturbance will dissipate after an initial transient. Mathematically this means that the wave speed is complex, i.e., $c = c_r + ic_i$ with $c_i > 0$ unstable. The stability of the shear layer will now be examined.

Rayleigh[10], in 1880, showed for inviscid incompressible flow that velocity profiles with inflection points are unstable. Recently, Michalke[11] confirmed that a shear layer is unstable but only at low frequencies ($\lambda/\delta > 2\pi$ or $f\delta 4\pi/U_\infty < 1$). It was felt that more information about the stability of a compressible shear layer was needed, therefore, a linear stability analysis was undertaken[12]. The governing Euler equations were linearized by assuming small perturbations caused by small amplitude traveling waves. The resulting stability equation first derived by Lees and Lin[13], reduces to the Rayleigh equation for incompressible flow.

$$a^2[g^{-1}(U - c)\phi_y - g^{-1} U_y \phi]_y = \alpha^2(U - c)\phi \qquad (9)$$

where

$$v = \phi(y)e^{i\alpha(x - ct)} \tag{10}$$

$$g = a^2 - (U - c)^2 \tag{11}$$

The eigenvalues of this Rayleigh equation were then computed[12] for a shear layer with a hyperbolic tangent velocity profile.

$$\frac{U}{U_\infty} = 0.5\ (1 + \tanh \frac{y}{\delta}) \tag{12}$$

The propagation velocity (c_r) of the disturbances is shown in Figure 3.

$$\frac{c_r}{U_\infty} = k \tag{13}$$

This is the k value determined experimentally by Rossiter[6] and found to be in excellent agreement with his results.

$$.5 < k < .6$$

The amplification factors ($c_i > 0$) were found to be a function of wave number (α) and Mach number (Figure 4). Instability was observed only for wave numbers less than unity. This implies short cavities ($L < 2\pi\delta$) will not resonate. Note the Rayleigh instability vanishes above M = 2.5. This result confirms previous experimental and numerical results that separated flows are more stable at supersonic speeds than at subsonic.

It is possible to predict the relative intensity of the different modes occurring in an open cavity. Consider a cavity of L = 91.44 cm and $M_\infty = 0.85$, $U_\infty = 286.5$ mps

Hence,

$$\frac{c_r}{U_\infty} = k = .52 \quad \text{(from Fig 3)}$$

$$M = 0.79$$

$$f = 115 \text{ (Hz)} \quad \text{Rossiter's Eqn.}$$

These different mode frequencies are plotted in Figure 5 using results of Ref 12, and the second mode is observed to have the greatest amplification while modes four and above are found to be stable. A spectral analysis of a wind tunnel test (Ref 14) for an open cavity at these same conditions is also shown in Figure 5. Observe that only the first four modes are dominant and the relative amplitudes of these four modes are consistent with the analytic amplification factors.

The intensity of the pressure fluctuation will be proportional to the following:

$$p_{rms}(M) \sim q(e^{\alpha c_i} - 1) \tag{14}$$

Selecting the peak value of $e^{\alpha c_i}$ for each Mach number and multiplying by $q/P_o(M)$ the relative intensity as a function of Mach number may be deduced (Fig 6). The peak pressure value occurring in a series of wind tunnel tests at different Mach numbers can be expected to occur near Mach one. This is confirmed in Reference 3 and 14.

IV. Summary of Analytic Results

The analytic results based primarily upon stability theory provide us with the following conclusions.

a. Shear layers (with inflection points in the velocity profile) are unstable but only for low frequencies; $f\delta/U_\infty < 1/4\pi$.

b. Short cavities ($L < 2\pi\delta$) will not resonate.

c. No Rayleigh instability occurs above Mach number 2.5.

d. Peak amplification occurs at about half the cut-off frequency creating a situation where modes other than the fundamental can dominate.

e. Maximum pressure intensity of a shear layer oscillation will occur near Mach 1 (in a wind tunnel with constant p_o).

Linear stability theory is therefore useful in explaining the cause of the resonance and in estimating the relative intensity of the various modes including the influence of Mach number. However, the full non-linear equations are required to determine the absolute level of the pressure intensity. For that reason the numerical solution of the unsteady Navier-Stokes equations will be considered next.

V. Numerical Computation

With the completion of the simplified analytic approach (ie, inviscid, linear stability theory) a numerical solution of the exact equations was attempted to further improve the prediction capability. The analysis served to identify the primary mechanism involved in the oscillation and greatly assisted in the determination of the grid point distribution and step sizes required to resolve the flow features.

A case to compute was selected for which experimental data were available. The test conditions of Heller and Bliss[3] were selected to compare the numerical computations (Figure 7).

$M = 1.5$	$L = 91.44$ cm
$L/D = 2.25$	$D = 40.64$ cm
$Re = 1.28 \times 10^6/m$	$\delta_o = 2.54$ cm

The width of the cavity was 22.86 cm and found not to be a major factor in the overall phenomenon. For this reason, a two-dimensional computation appeared to be justified for the initial studies.

VI. Governing Equations

The time dependent explicit finite difference method originated by R. MacCormack[15] was selected to perform the numerical calculations. The two-dimensional Navier-Stokes equations follow:

$$\frac{\partial U}{\partial t} + \frac{\partial E}{\partial x} + \frac{\partial F}{\partial y} = 0 \tag{15}$$

$$U = \begin{vmatrix} \rho \\ \rho u \\ \rho v \\ \rho e \end{vmatrix} \quad ; \quad E = \begin{vmatrix} \rho \\ \rho u^2 - \sigma_{xx} \\ \rho uv - \tau_{xy} \\ \rho ue - \sigma_{xx} u - v\tau_{xy} - \dot{q}_x \end{vmatrix} \quad ; \tag{16}$$

$$F = \begin{vmatrix} \rho v \\ \rho uv - \tau_{xy} \\ \rho v^2 - \sigma_{yy} \\ \rho ve - v\sigma_{yy} - u\tau_{xy} - \dot{q}_y \end{vmatrix}$$

where

$$\sigma_{xx} = -p - 2/3\mu\nabla \cdot \bar{u} + 2\mu u_x$$

$$\tau_{xy} = \mu(u_y + v_x)$$

$$\sigma_{yy} = -p - 2/3\mu\nabla \cdot \bar{u} + 2\mu u_y$$

The turbulent closure of the present problem was achieved by implementing the Cebeci-Smith eddy viscosity model with relaxation modification[16]. The relaxation turbulence model was used in an attempt to describe the adjustment of the turbulence structure from an attached boundary layer to an oscillatory free shear layer. The relaxation length scale was assigned a value of 55 boundary layer thicknesses. Since there is no guidance to

assess the accuracy of the turbulence model relative to low frequency fluctuations, a parametric study seemed to be necessary. In the present analysis, several consecutive calculations with suppressed eddy viscosity were performed and the numerical results exhibited only a minor departure from the basic solution. Hence, the present eddy viscosity model was felt to be adequate. The computer program previously used by Shang[16,17] was modified to include the appropriate boundary conditions for this problem.

VII. Boundary Conditions

Four faces require attention in the specification of boundary conditions (Figure 7).

Wall and Cavity Surfaces:

On solid surfaces, the velocity components vanish, and the wall temperature must be prescribed. In addition, the pressure is derived from the respective compatibility conditions of the momentum equations.

$$u = 0 \qquad v = 0 \qquad T_w = T_0$$

$$\frac{\partial p}{\partial x} = \frac{\partial}{\partial x}\left[-2/3\mu\nabla\cdot\bar{u} + 2\mu u_x\right] - \frac{\partial}{\partial y}\left[\mu(u_y + v_x)\right]$$

$$\frac{\partial p}{\partial y} = \frac{\partial}{\partial y}\left[-2/3\mu\nabla\cdot\bar{u} + 2\mu u_y\right] - \frac{\partial}{\partial x}\left[\mu(u_y + v_x)\right] \qquad (18)$$

Upstream Condition:

A supersonic free stream with a known boundary layer profile is given.

$$u = u(y) \qquad T = T_0 - \frac{u^2}{2C_p}$$

$$v = 0 \qquad p = p_\infty \qquad (19)$$

Downstream Condition:

A mild boundary condition is prescribed to avoid major reflections of disturbances.

$$\frac{\partial u}{\partial x} = 0 \qquad \frac{\partial T}{\partial x} = 0$$

$$\frac{\partial v}{\partial x} = 0 \qquad \frac{\partial p}{\partial x} = 0 \tag{20}$$

Upper Boundary:

A similar no-reflection condition is adopted.

$$\frac{\partial u}{\partial \zeta} = 0 \qquad \frac{\partial T}{\partial \zeta} = 0$$

$$\frac{\partial v}{\partial \zeta} = 0 \qquad \frac{\partial p}{\partial \zeta} = 0 \tag{21}$$

Where ζ is the outgoing characteristics on the upper boundary of the computational domain.

Initial Condition:

The upstream condition is imposed as the initial condition for the flow outside the cavity. Inside the cavity initially the flow is assumed to be static.

$$u = 0 \qquad v = 0 \qquad T = T_o \qquad p = p_\infty \tag{22}$$

VIII. Numerical Procedure

MacCormack's[15] alternating-direction-explicit numerical scheme was adopted for the present analysis. For this case pressure damping was required due to the transient multi-wave structure occurring in the flow

field. The current philosophy in computational fluid dynamics is to employ a body oriented coordinate system which turns out to be Cartesian in this case with non-uniform step size. For cases presented here, a grid of 78 x 52 was used to represent a field size of 182.9 cm x 91.44 cm enclosing a 91.44 cm x 40.64 cm cavity (see Figure 7). In order to achieve the desired temporal resolution, a time step corresponding to a Courant number of 0.2 was used. All calculations were performed on a CDC 6600 computer. The data processing rate was 0.0017 sec per grid point per time step. The central core memory required for the present problem is 205K octal.

Although dispersion, dissipation and phase errors are not negligible with the step sizes employed, previous numerical investigations of viscous interaction problems[15,16] using comparable step sizes have shown good agreement (± 5% with experimental data for the most significant features of the flow. In particular, periodic motions around a transonic airfoil have been studied by Levy[18] with a basic MacCormack's scheme. His results exhibited good agreement with experimental data not only in the pattern of a simple wave train but also in the predicted reduced frequency. Therefore, no additional modification other than a simple controlled spatial averaging was used to correct the possible dispersion error for the compound wave problem investigated.

IX. Discussion of Results

Time dependent numerical computations of supersonic flow over an open cavity were accomplished utilizing MacCormack's finite difference explicit method. The entire velocity field over the cavity is shown in

Figure 8. Since the problem is strictly a time dependent phenomenon, only a typical velocity distribution is presented here (t = 0.0062 sec) to reveal the basic features. The most obvious feature is that the flow field within the confined cavity is subsonic, except perhaps the region adjacent to the cavity opening. The experimental investigation[3] also recorded the identical observation. The orderly development of the shear layer above the cavity is also clearly exhibited. An attached turbulent boundary layer upstream of the cavity separates at the forward bulkhead to form a free shear layer over the cavity and finally reattaches downstream of the cavity. Due to the smaller magnitude of the velocity components within the cavity, the velocity distribution could not be shown with the same scale as that of the outer shear layer. A magnified velocity profile in the cavity is presented in Figure 9. All velocity distributions were drawn at a scale ten times greater than that in Figure 8. A recirculation flow configuration is demonstrated with the center of the recirculation located near the upper corner of the rear bulkhead. For clarity only every fourth velocity point in the streamwise direction was presented in both figures (Fig 8 and 9).

A quantitative comparison of the calculated mean velocity distribution with experiment is presented in Figure 10. The calculated velocity profile immediately upstream and downstream of the cavity compares very well with the experimental measurements. The upstream velocity profile is essentially independent of time as expected, and nearly duplicates the data. The downstream velocity profile indicates that the reattached shear layer thickens significantly over the cavity. The difference between data and calculation is a mere seven percent. The computed velocity profile downstream of the cavity exhibits an oscillatory behavior in the inner portion of the boundary layer which is confirmed by the experimental observation.

A comparison of the time-average surface pressure distribution in the cavity was performed. In Figure 11, one observes that the computed mean pressure, normalized by the free stagnation pressure, uniformly under predicts the experimental data[3] by about 10 percent. The maximum deviation between data and calculation occurs near the rear bulkhead were the pressure difference accross the cavity opening and cavity floor also reaches a maximum. Nevertheless, the calculated results indicate the identical trend to that of the experiment[3].

In Figure 12, a history of the static pressure at $x/L = 0.66$ and $y/L = 0.960$ is monitored ($y/L = 0.960$, $x/L = 0.33$, 0.50 and 0.66). Persistent oscillatory static pressures appeared within one characteristic time, t_{ch}. The characteristic time is defined as the period of time required for a fluid particle to traverse the length of the cavity at freestream speed. For the present problem t_{ch} has a value of 1.987×10^{-3} seconds. Since the pressure oscillation over the cavity is composed of several frequencies of different amplitude, a compound wave system develops. The present calculation was carried out only over a time span of about nine characteristic times ($t = 1.82 \times 10^{-2}$ secs). This result is compared with oscillogram data for the test results of Ref. 18 in Figure 12. In order to permit a qualitative comparison, computed results are repeated for several cycles. One can detect certain similarity between the data and the present result. In principle, the solid surface constraint and wave interference phenomenon of the present problem are inherently nonlinear. Therefore, caution must be exercised in discerning the discrete frequencies between the fundamental modes of oscillation. Other basic information such as the relative phase angle and the amplitude of each distinctive wave requires further spectral analysis.

A spectral analysis of this compound wave probably is the only reliable means for accurately obtaining mode frequency. However, this is impractical due to the large amount of computer time required to obtain solutions for a sufficiently long duration. Hence, an analysis was accomplished by assuming the waves to be commensurable. The spectral analysis reveals four distinctive discrete frequencies of 154 Hz, 308 Hz, 462 Hz, and 616 Hz recognized as the first, second, third and fourth mode respectively of the oscillatory pressure disturbance. The higher modes of oscillation decay rapidly as one may observe in Figure 13. Good agreement between the experimental measurement and present result is observed. Both exhibit a dominate second mode of the pressure oscillation. The level of pressure oscillation in db can be evaluated as

$$p(db) = 20 \log \frac{p_{rms}}{q_\infty} + 189$$

where q_∞ is the dynamic pressure (54 K pascal). The detected frequency for the second mode (308) compares well with the experimental data (300 Hz) and Rossiter's prediction[6] (328 Hz). The fluctuating pressure level between the data and present result is within about ten percent.

The compound wave pattern is best illustrated in Figure 14. The propagation of the wave train from the forward bulkhead is presented for a fixed time interval of 0.64×10^{-3} seconds. One observes the rearward traveling propagation wave has an unmodulated amplitude until interacting with reflected waves from the rear bulkhead. No repeatable wave front can be identified downstream of $x/L = 0.75$. Two pieces of important information have been determined from this graph, namely the rearward wave propagation speed and the amplitude of the pressure oscillation. The predicted wave speed has a value of 244.4 mps (or $k = .53$) and is in agreement

with the predicted value from Figure 3. The amplitude of the oscillating pressure also agrees well with data, ($\pm$ 6.464 K pascal vs 7.182 K pascal; or 170 db) with the discrepancy about 10%.

In Figure 15 the sequence of density contours from the numerical computation is shown for a complete cycle of the periodic motion. The forward and rearward moving wave system originated from the instability of the free shear layer and the reflection at the rear bulkhead can be easily recognized in the cavity. The generation and movement of the external shock wave system also can be recognized. These compare favorably with the wave pattern shown in Figure 1 for the water table experiment.

X. Conclusions

The pressure oscillation for supersonic flow over an open cavity has been predicted by numerically solving the unsteady Navier-Stokes equations. Both the predicted frequency and magnitude of the unsteady pressure fluctuations were qualitatively confirmed through experiment. However, a spectral analysis of a numerical solution of longer duration is required for complete verification. This is the first time a complete viscous solution of the pressure oscillating cavity has been obtained and displays the outstanding capability inherent in the numerical methods of today.

References

1. Krishnamurty, K., "Acoustic Radiation from Two Dimensional Rectangular Cutouts in Aerodynamic Surfaces," NACA TN 3487, August 1955.

2. Heller, H., Holmes, G. and Covert, E., "Flow Induced Pressure Oscillations in Shallow Cavities," AFFDL-TR-70-104, WPAFB, Ohio, 1970.

3. Heller, H. and Bliss, D., Aerodynamically Induced Pressure Oscillations in Cavities: Physical Mechanisms and Suppression Concepts, AFFDL-TR-74-133, WPAFB, Ohio, 1974.

4. Clark, R. L., "Weapons Bay Turbulence Reduction Techniques," AFFDL-TM-75-147, WPAFB, Ohio, 1975.

5. Mainquist, R. S., "An Experimental Investigation into the Suppression of Flow-Induced Pressure Oscillations in Two Dimensional Open Cavities," AFIT Thesis, March 1978.

6. Rossiter, J. E., "Wind-Tunnel Experiment on the Flow Over Rectangular Cavities at Subsonic and Transonic Speeds, R & M No. 3428, British A.R.C., October 1964.

7. Spee, B. M., "Wind Tunnel Experiments on Unsteady Cavity Flow at High Subsonic Speeds," AGARD Conference Proc., No. 4, Separated Flow II, 1966.

8. Quinn, B., "Flow in the Orifice of a Resonant Cavity," AIAA Student Journal, 1963.

9. Borland, C. J., "Numerical Prediction of the Unsteady Flowfield in an Open Cavity," No. 77-673, AIAA 10th Fluid & Plasma Dynamics Conference, 1977.

10. Rayleigh, Lord, "On the Stability or Instability of Certain Fluid Motion," Scientific Papers, Vol. 1, pp. 474-484, 1880.

11. Michalke, .A, "On the Inviscid Instability of the Hyperbolic-Tangent Velocity Profile," Journal Fluid Mechanics, Vol. 19, pp 543-556, August 1964.

12. Roscoe, D. and Hankey, W., "Stability of Compressible Shear Layers," (To be published as an AFFDL-TR, 1978).

13. Lees, L. and Lin, C.C., "Investigation of the Stability of the Laminar Boundary Layer in a Compressible Fluid," NACA TN 1115, Sep 1946.

14. Maurer, O., "Investigation and Reduction of Weapons Bay Pressure Oscillations Expected in the B-1 Aircraft," AFFDL-TM-74-101, WPAFB, Ohio, 1974.

15. MacCormack, R. W. and Baldwin, B. S., "A Numerical Method for Solving the Navier-Stokes Equations with Application to Shock Boundary Layer Interactions," AIAA Paper 75-1, Pasadena, California, 1975.

16. Shang, J. S. and Hankey, W. L., Jr., "Numerical Solutions for Supersonic Turbulent Flow over a Compression Ramp," AIAA J., Vol. 13, Oct 1975.

17. Shang, J. S. and Hankey, W. L., Jr., "Numerical Solution of the Navier-Stokes Equations for a Three-Dimensional Corner," AIAA J., Vol. 15, 1977, pp. 1575-1582.

18. Levy, L. L., Jr., "Experimental and Computational Steady and Unsteady Transonic Flows About a Thick Airfoil," AIAA J., Vol. 16, No. 6, June 1978, pp. 564-572.

Figure 1. Typical Pressure Oscillation Cycle (Ref. 3)

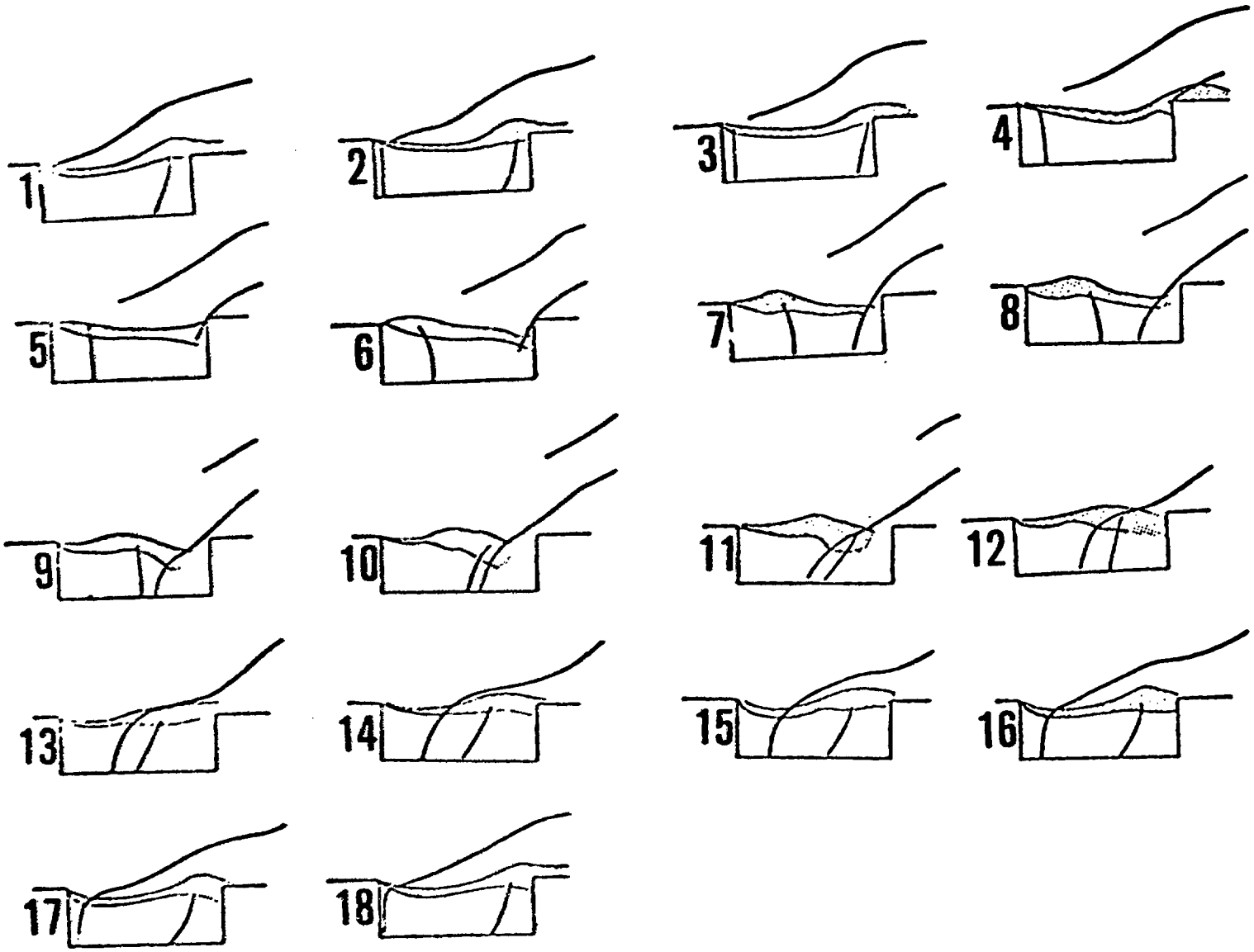

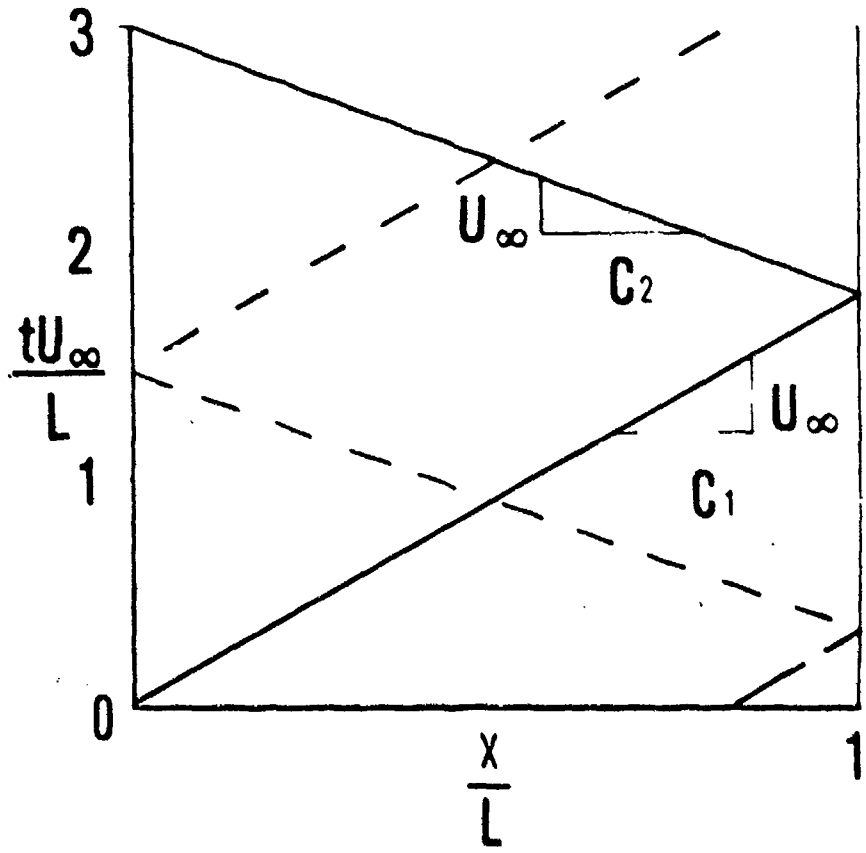

Figure 2. Wave Diagram

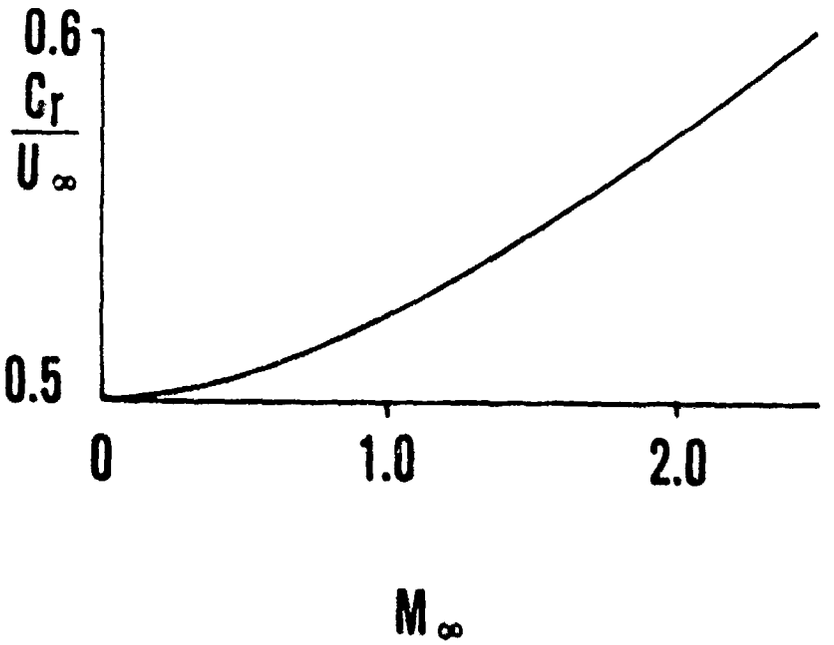

Figure 3. Propagation Velocity v.s. Mach Number of Traveling Waves in a Free Shear Layer (Ref. 12)

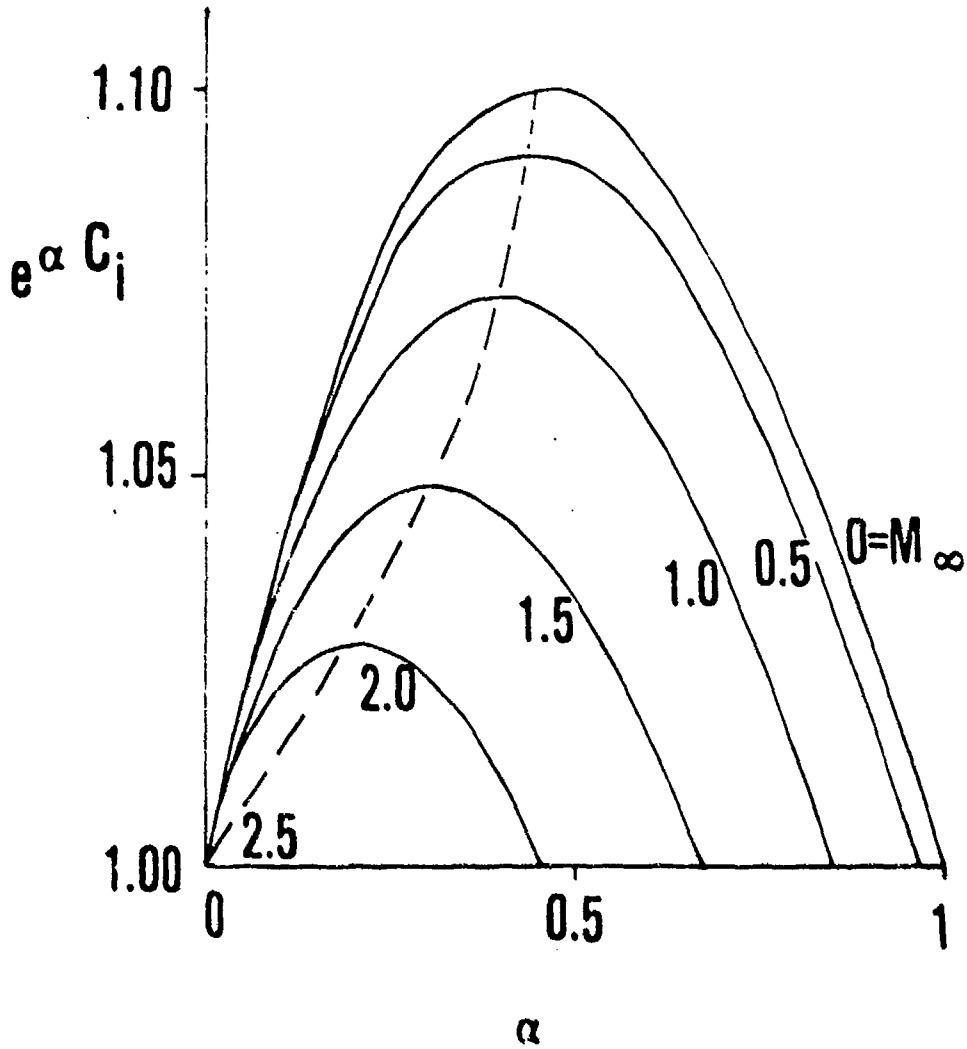

Figure 4. Amplification Factor v.s. Wave Number for Different Mach Number (Ref. 12)

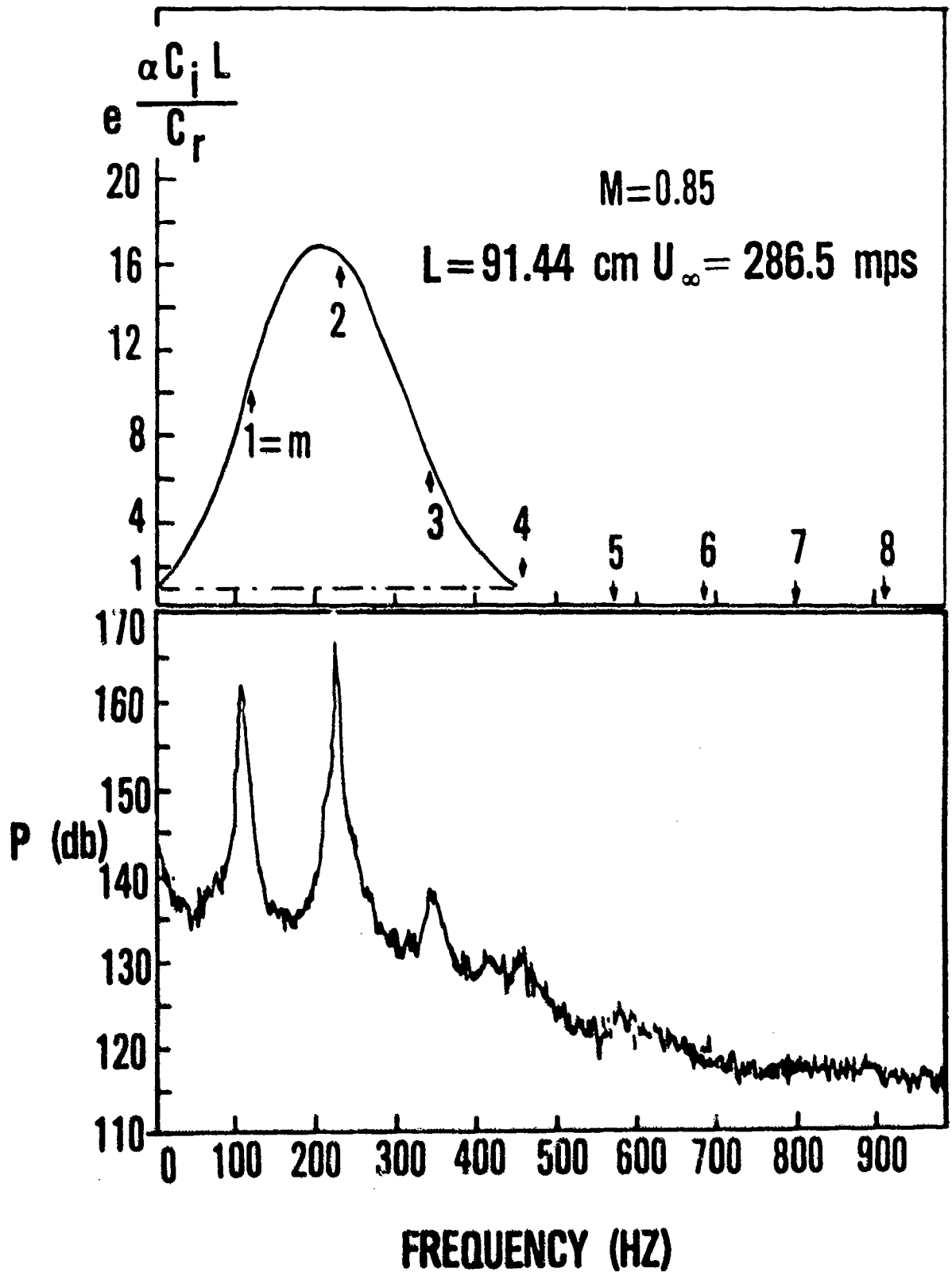

Figure 5. Comparison of Amplification for Different Frequencies with Experimental Data

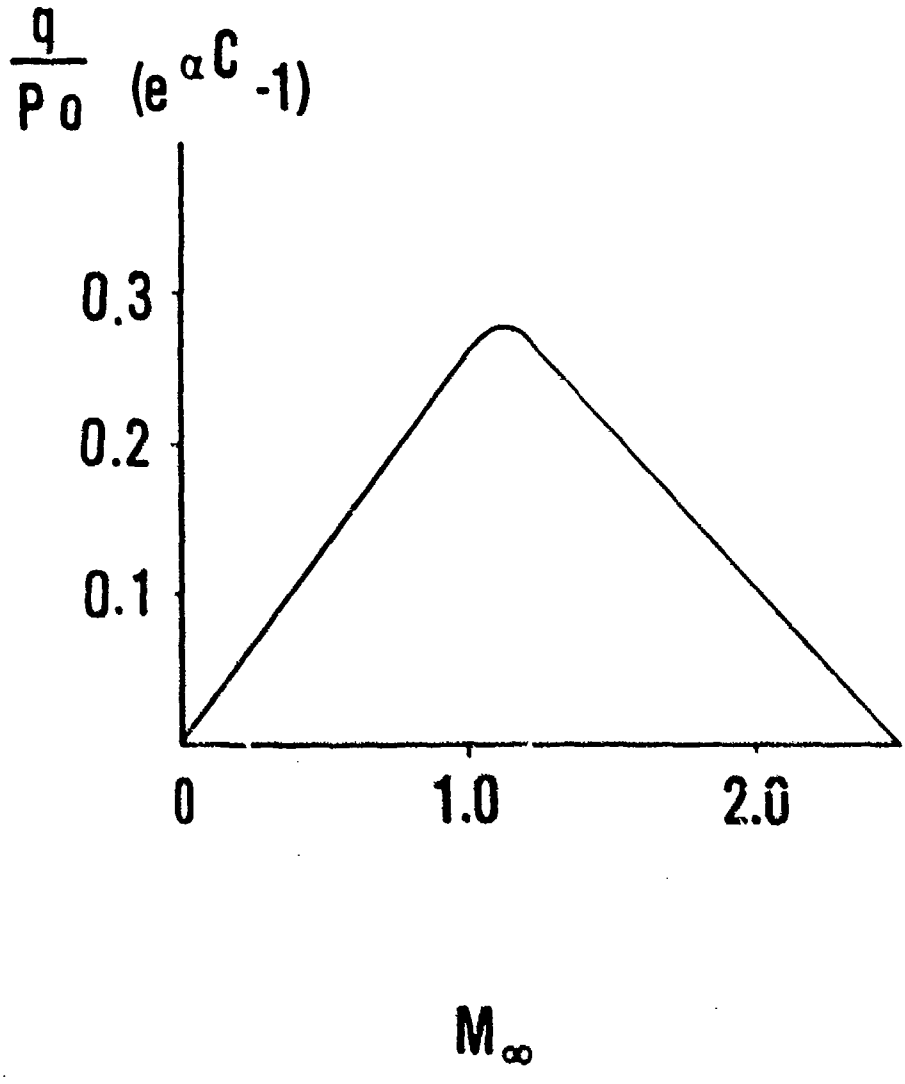

Figure 6. Relative Intensity of Disturbances for Different Mach Numbers

FIGURE 7. COMPUTATIONAL DOMAIN AND MESH POINT DISTURBATION FOR NUMERICAL INVESTIGATION

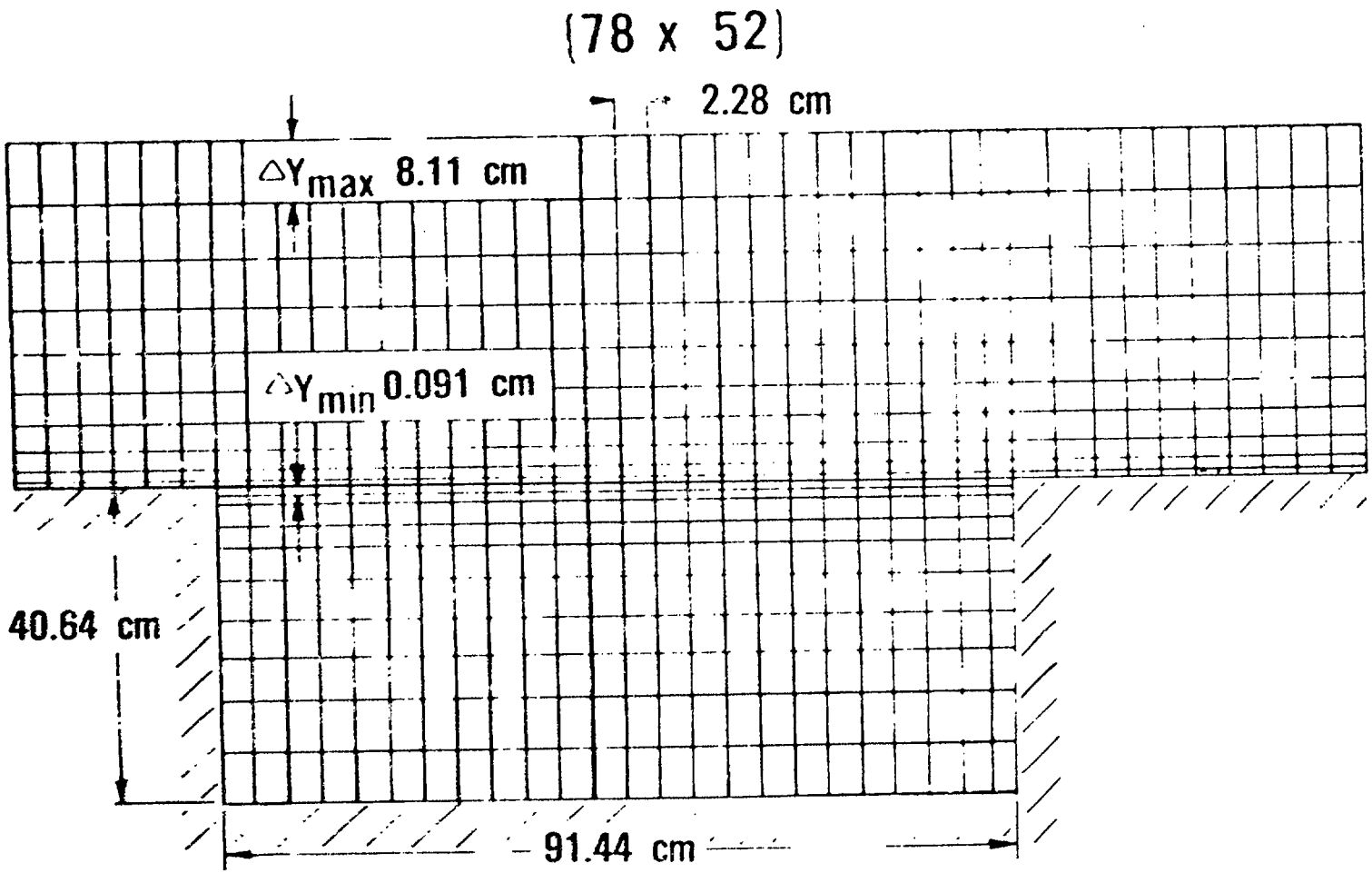

M_∞=1.50 Re=26×10^6 L/D=2.25

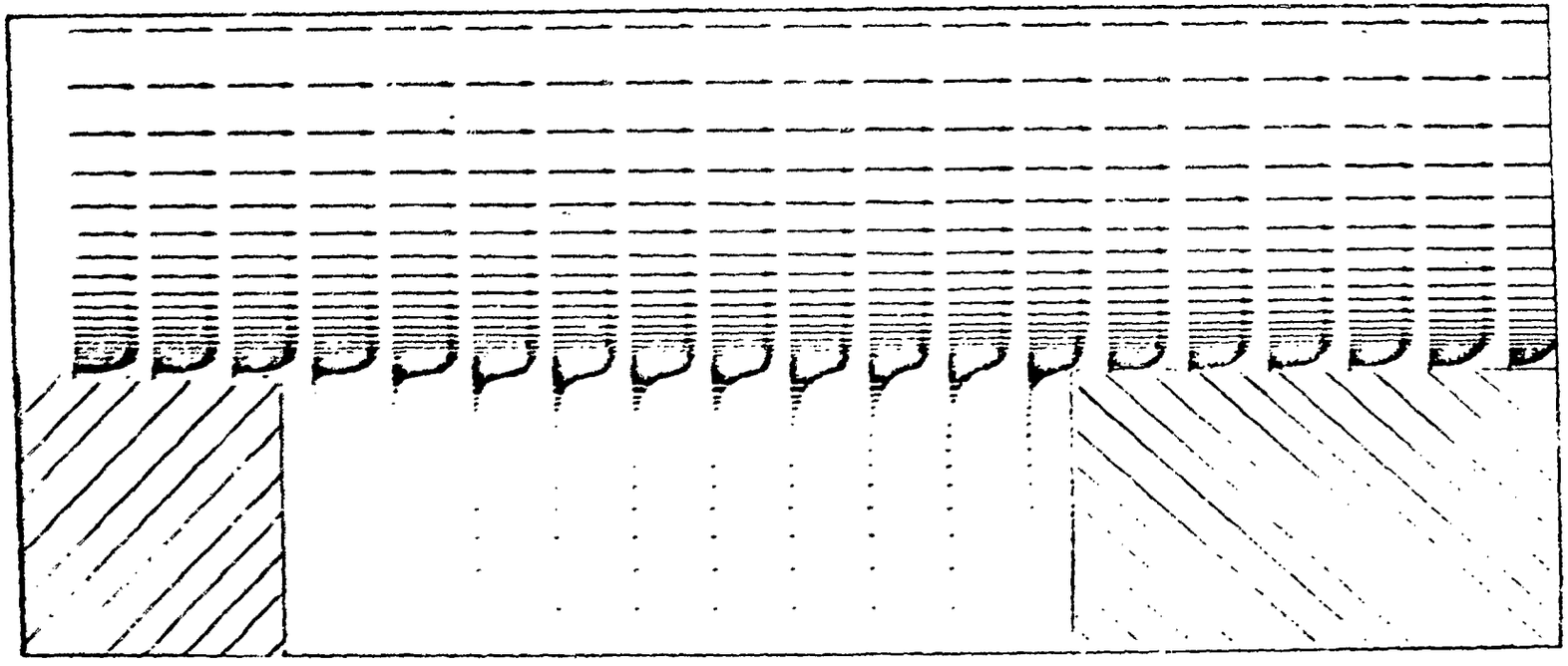

Figure 8. Velocity of the Entire Flow Field (t = 3tch)

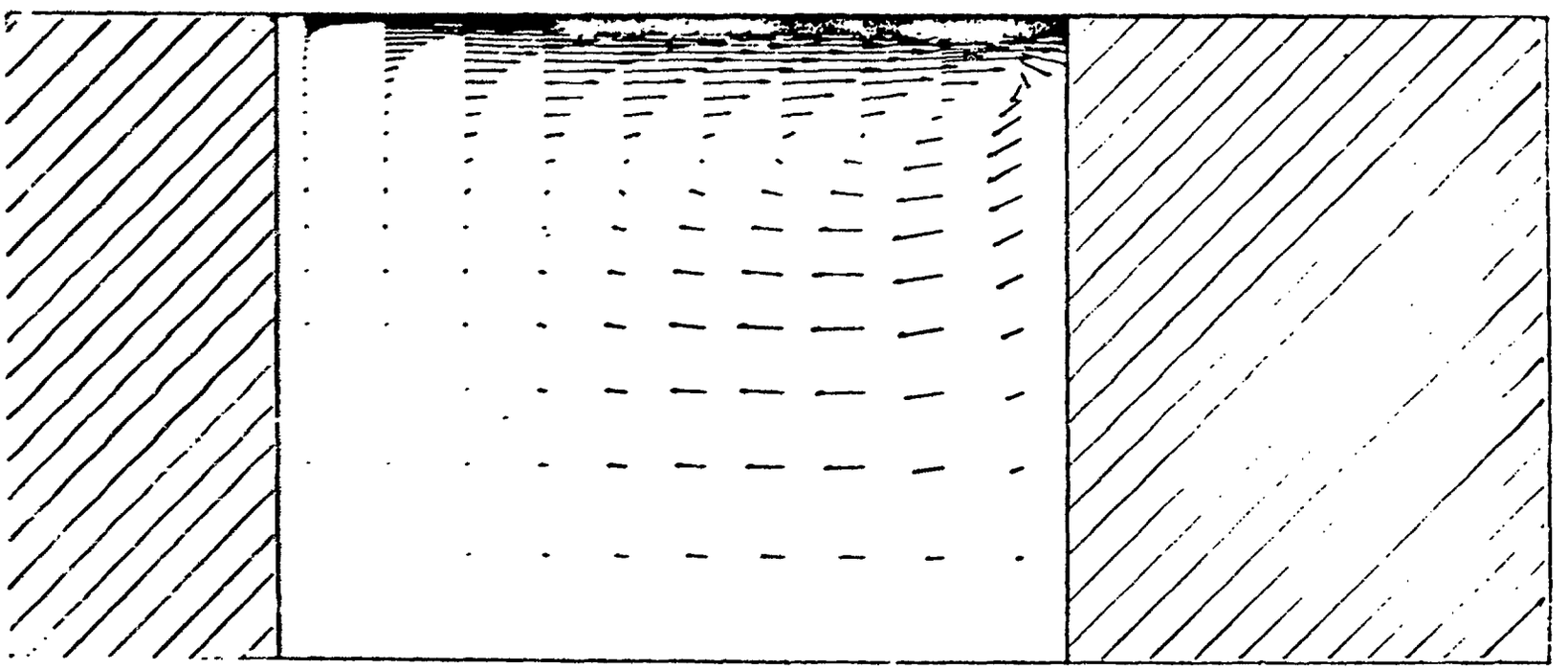

Figure 9. Velocity Profiles within the Cavity (t = tch)

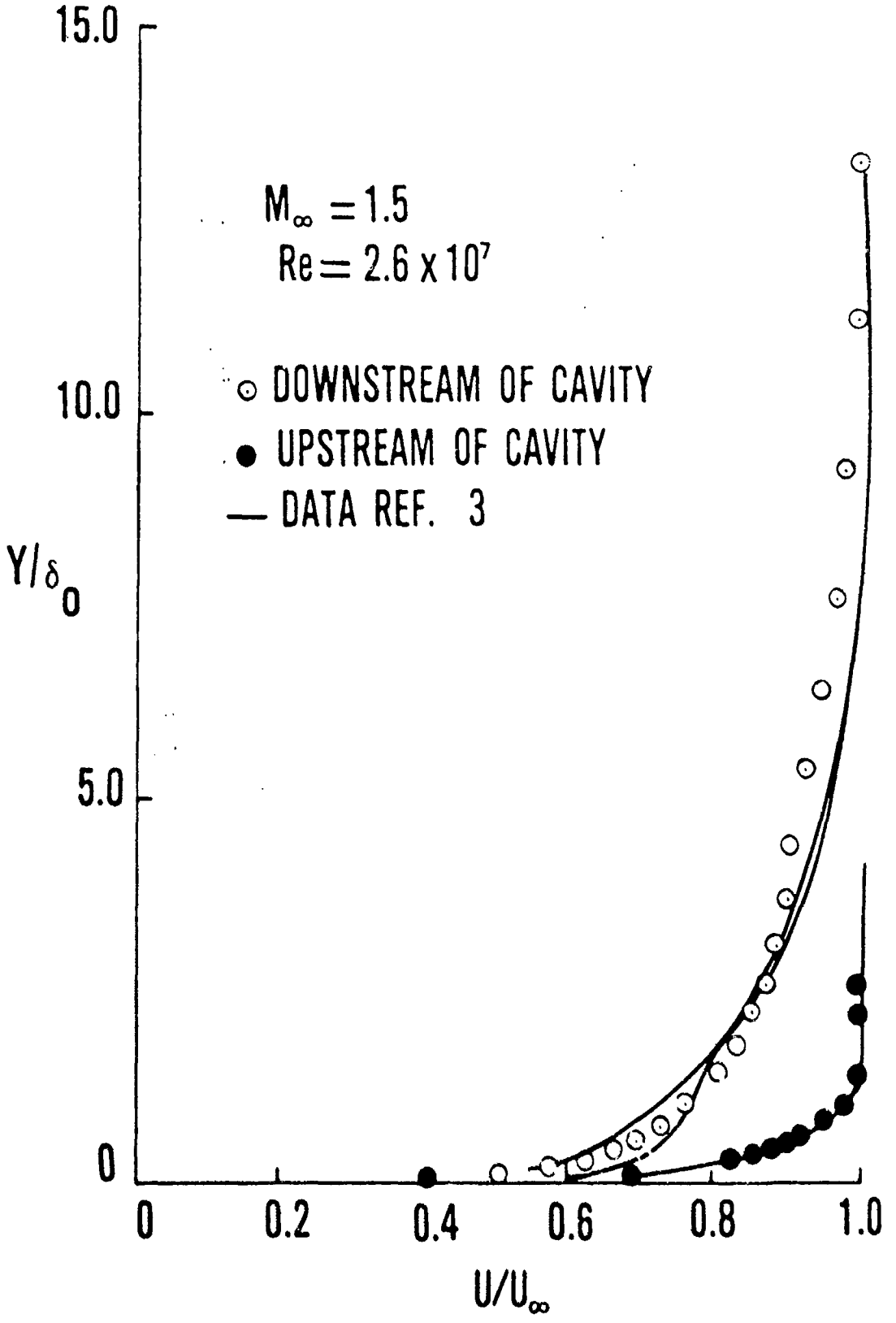

Figure 10. Comparison of Velocity Profiles

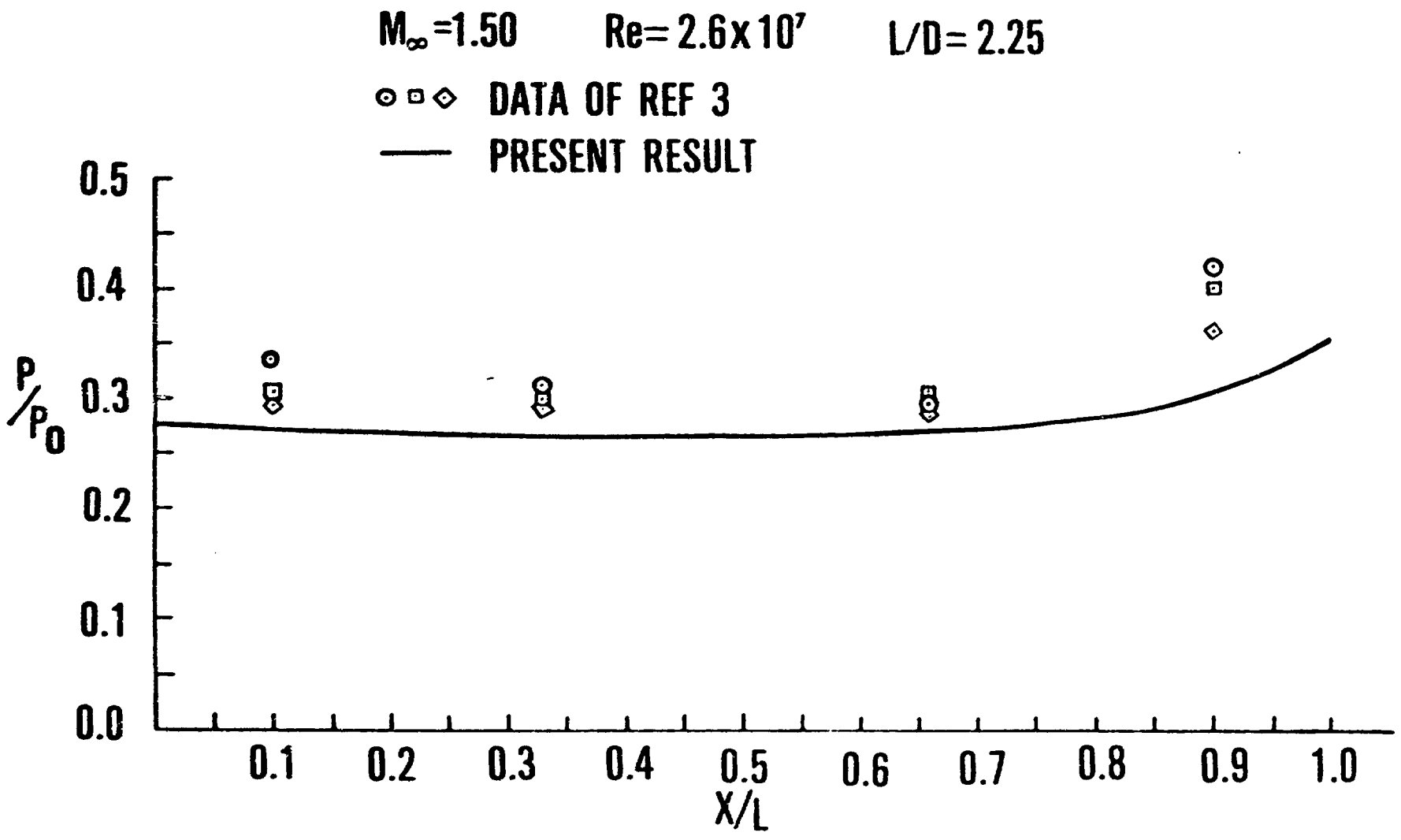

Figure 11. Comparison of Mean Static Pressure Over the Cavity

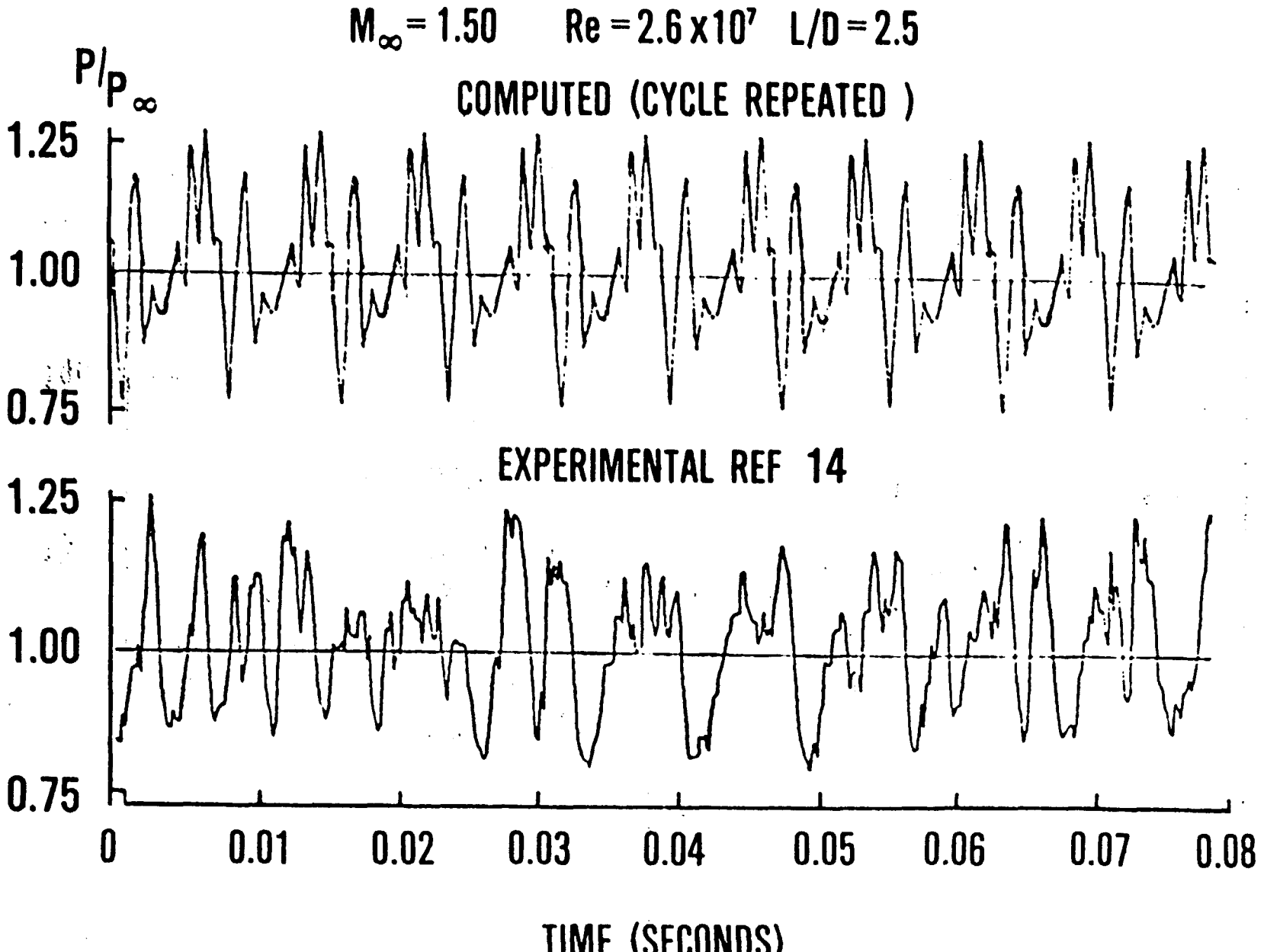

Figure 12. Pressure History in the Cavity

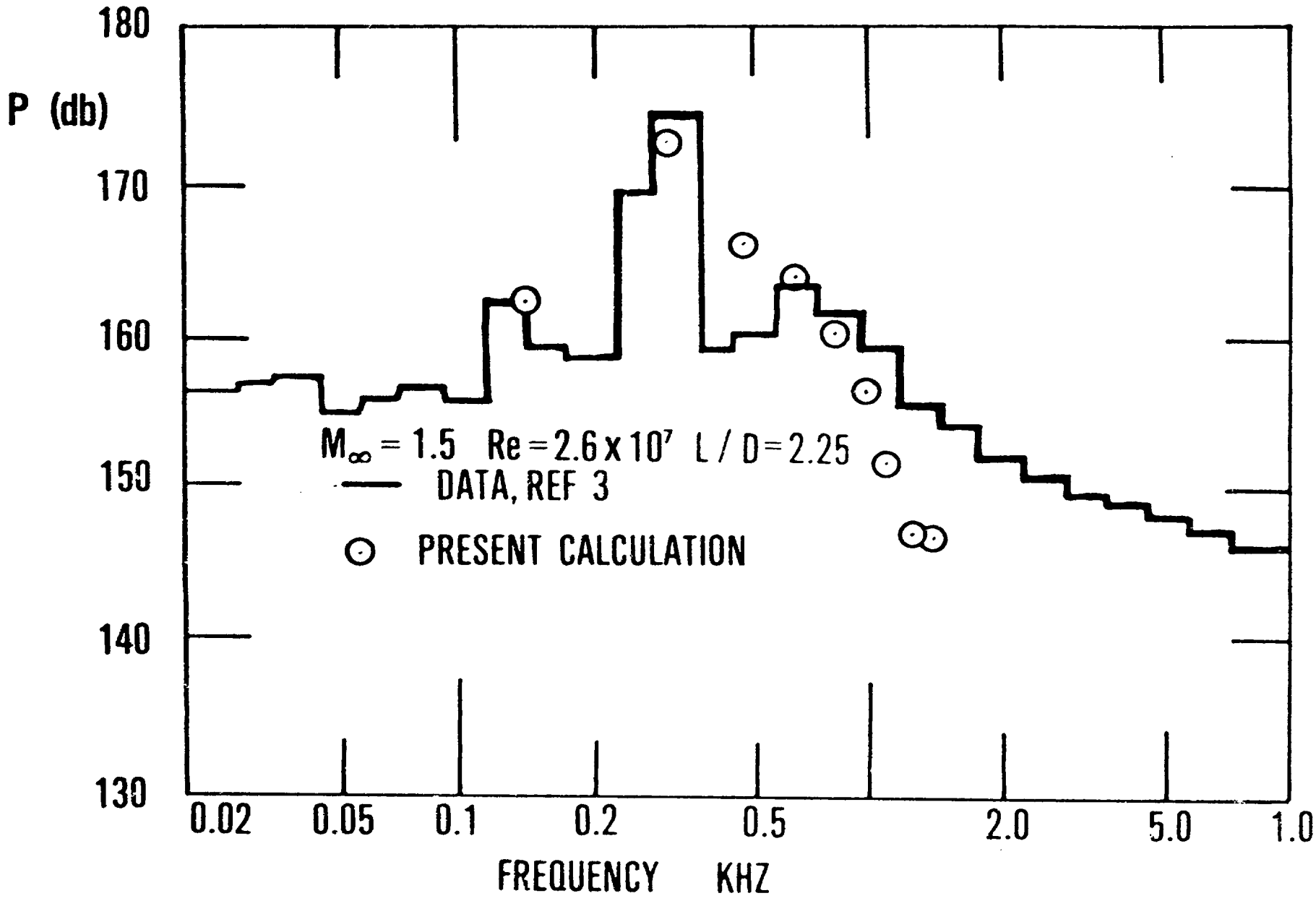

Figure 13. Comparison of Spectral Analysis Results

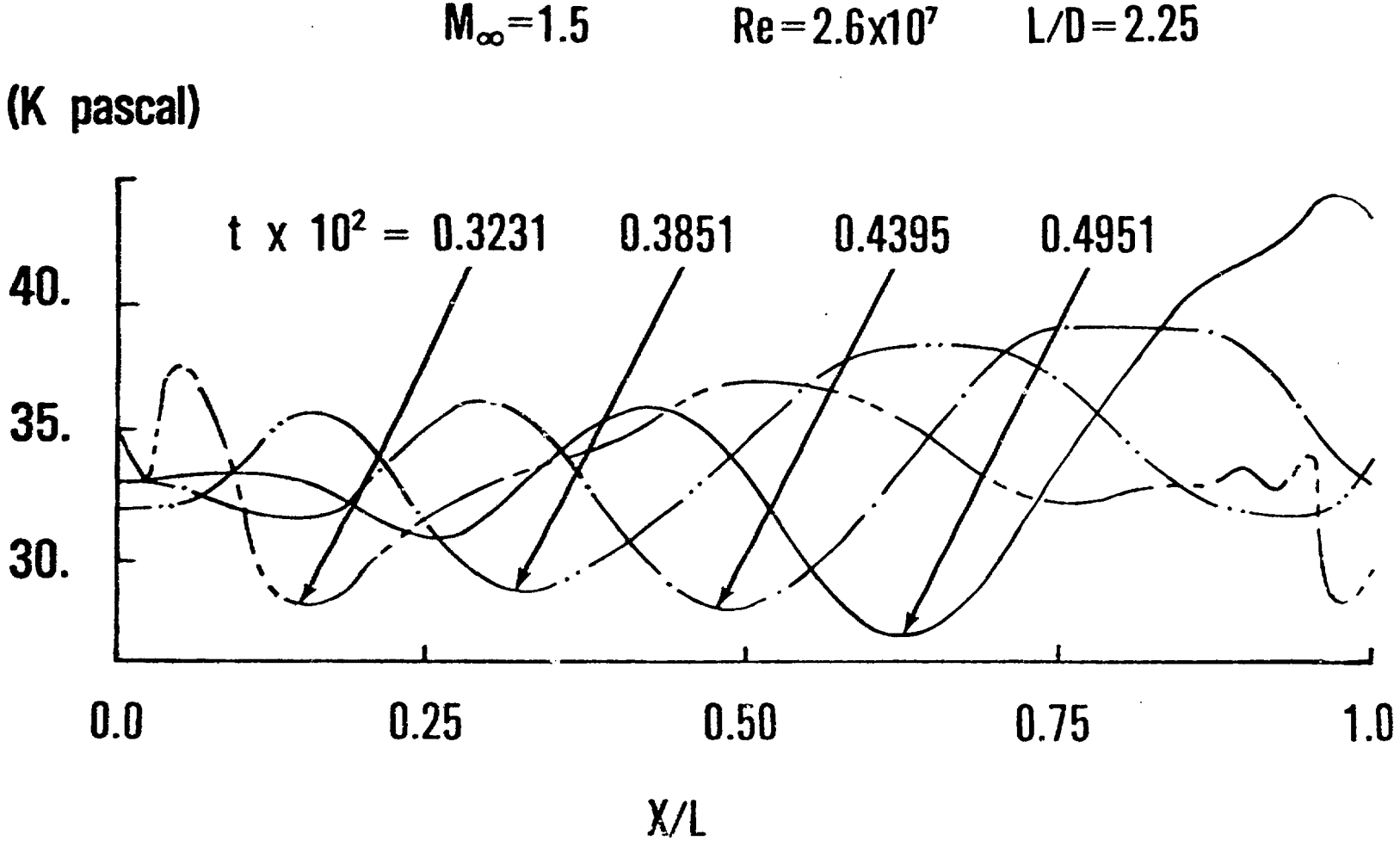

FIGURE 14. CAVITY WAVE PATTERN

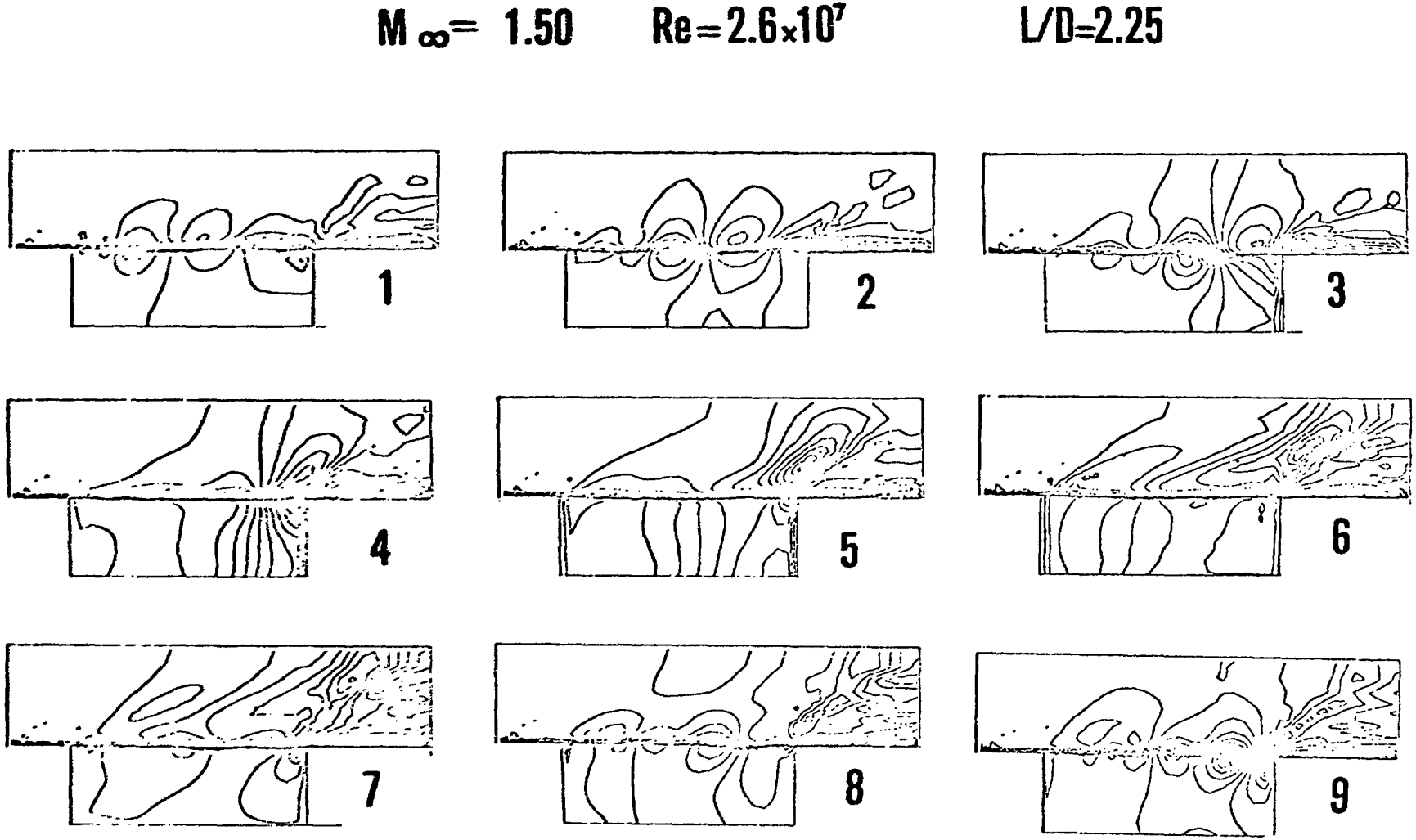

Figure 15. Sequence of Density Contour